

## ACTIVITIES AT THE LINAC4 TEST STAND

J-B. Lallement<sup>†</sup>, V. Bencini, S. Bertolo, F. Di Lorenzo, J. Lettry, A. M. Lombardi,  
 C. Mastrostefano, D. Noll, M. O'Neil,  
 CERN, Geneva, Switzerland

### Abstract

Linac4, the new CERN H<sup>-</sup> injector to the Proton Synchrotron Booster, has been commissioned and has delivered a beam intensity and quality calculated to be sufficient to produce the standard beams for LHC and the high intensity beams for ISOLDE when connected. The beam current is nevertheless half of what is foreseen and the problem has been identified at the low energy end, between the extraction and the matching to the RFQ. The Linac4 test stand is being used to address this issue by testing different extraction geometries and different plasma generators. A fast method to access the current in the RFQ acceptance has been put in place. This paper reports the results of the measurements obtained so far.

### INTRODUCTION

Linac4 is a 160 MeV H<sup>-</sup> normal conducting linear accelerator that is about to replace the present Linac2 as injector to the whole CERN proton accelerator complex. After a staged commissioning successfully completed in fall 2016, the linac underwent several test runs in 2017 and 2018 during which its performance, reliability and availability were recorded and optimized [1]. Linac4 has met all the required beam quality parameters needed for creating the various beams that the PSB is currently producing from the LHC beams to the fixed-target experiments beams. This is possible with a beam intensity of 25 mA, which represents 60% of the nominal intensity (40 mA). Nevertheless, to open the door to higher intensity in the CERN complex a current of 40 mA is needed. The intensity limitation comes from the pre-injector because the emittance of a 50mA beam from the present source exceeds the RFQ acceptance. For the present source a maximum current of 25 mA falls in the RFQ acceptance. A dedicated test stand, in operation for source development since 2008, is now dedicated to addressing this issue.

### THE LINAC4 TEST STAND

The Linac4 pre-injector is made of a RF source, which can provide a 600  $\mu$ s, 50 mA H<sup>-</sup> beam at 45 keV with a maximum repetition rate of 2 Hz, and a 352MHz, 3 m long Radio Frequency Quadrupole, bunching and accelerating the beam to 3 MeV. Acceleration is loss-less from 3 MeV onwards and no emittance growth has been observed for peak currents up to 25 mA. The 45 keV beam extracted from the source is matched to the RFQ via a Low Energy Beam Transport line housing 2 magnetic solenoids, an electrostatic pre-chopper, two steerers, a mechanism to inject different gases to influence neutralisation and a beam

current transformer and time resolved profile harps for diagnostics.

The Linac4 set-up is not suitable for in-depth studies and source tests. Therefore, a replica of the Low Energy Beam Transport has been assembled at a dedicated test stand, which is equipped with extra diagnostics including a slit-and-grid, time resolved emittance meter, a Faraday cup and profile harps. A very effective procedure to reconstruct a sample beam from emittance measurements has been described in [2] and it has been extensively used to estimate the number of particles falling into the RFQ acceptance and the matching conditions. In parallel a more rapid method has been put in place. This method is based on simulating the RFQ acceptance by a series of four transverse collimators (the mask) and obtaining the current into the RFQ acceptance by measuring the current with a Faraday cup placed downstream. This method, besides being faster, is more suitable for an automatic optimisation of the LEBT parameters (focusing and steering). The layout of the test stand is show in Fig. 1.

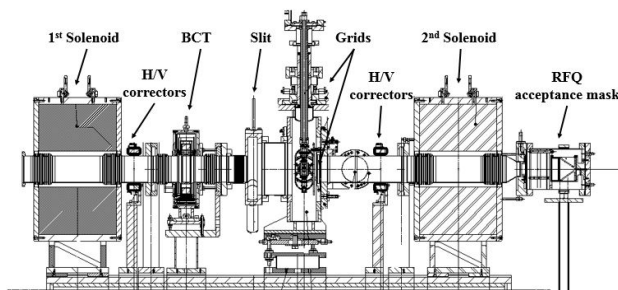


Figure 1: Linac4 test-stand layout.

### The RFQ Acceptance Mask

The RFQ acceptance mask device is made of four inter-cepting plates with squared aperture restrictions. The aperture size and their relative distances are chosen such that only the particles within the RFQ acceptance can pass through all four aperture restrictions. Extensive calculation under different regimes of space charge distribution and intensity have been performed to validate this device.

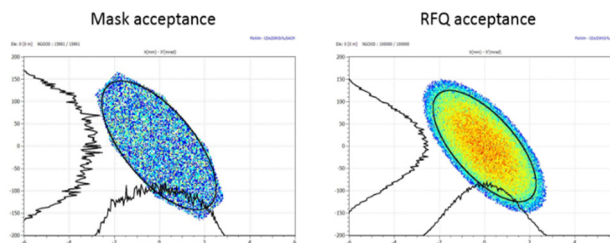


Figure 2: Comparison between the Linac4 RFQ and the mask transverse acceptances at zero current. Mask acceptance on the left, RFQ acceptance on right.

<sup>†</sup> jean-baptiste.lallement@cern.ch

Content from this work may be used under the terms of the CC BY 3.0 licence (© 2018). Any distribution of this work must maintain attribution to the author(s), title of the work, publisher, and DOI.

A comparison between the Linac4 RFQ acceptance as obtained by the code PARMTEQ [3] and the mask acceptances is shown in Fig. 2. The areas and the orientation of the two acceptances ellipses are very similar. As the mask is built with a finite number of aperture restrictions, the edges of the mask acceptance are sharp. The phase advance between the four plates is chosen close to 45° such that the cuts are uniformly distributed around the ellipse.

In order to validate the mask prediction, a variety of beam distributions were simulated through both the Linac4 RFQ and the mask using PARMTEQ [3] and Toutatis [4] for the RFQ simulations and Travel [5] and TraceWin [6] for the mask. In all the tested cases, the mask gives a slightly higher transmission than the RFQ (the highest overestimation is 5%). This discrepancy can be explained as the mask only reproduces the transverse losses, and not the longitudinal losses that occur in the RFQ during the bunching and acceleration processes. It is nevertheless a good guideline for the quality of a source. A sketch of the RFQ acceptance mask is shown in Fig. 3.

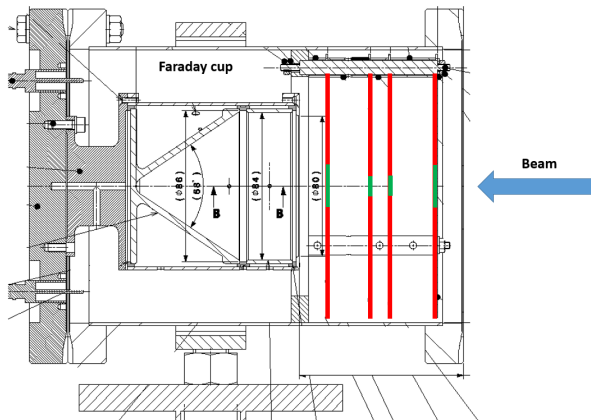


Figure 3: RFQ acceptance mask layout. The intercepting plates in red, with square holes in green (not on scale) are located upstream of a Faraday cup.

### IS03 SIMULATION AND MEASUREMENT

The H<sup>-</sup> ion source of Linac4 consists of a plasma generator driven by a 2 MHz RF at powers up to 100 kW, and the extraction system shown in Figure 4. Further information on the plasma generator and on the design of the extraction system can be found in [7, 8].

A puller-dump electrode at nominally 10 kV relative to the source, extracts the H<sup>-</sup> beam along with a significant amount of electrons. Depending on the mode of operation, the ratio between electrons and ions is in the range of 10 to 50 (volume mode). If a small amount caesium is evaporated into the plasma chamber (surface mode), this ratio can be reduced to around one. The puller-dump electrode houses a set of magnets that deflects the electron beam into a cup set into the side of the electrode. Electron currents up to 3 A can be dumped.

After the electrons are dumped, the beam is accelerated to the full energy of 45 keV and additionally focussed by an einzel lens at voltages up to 30 kV.

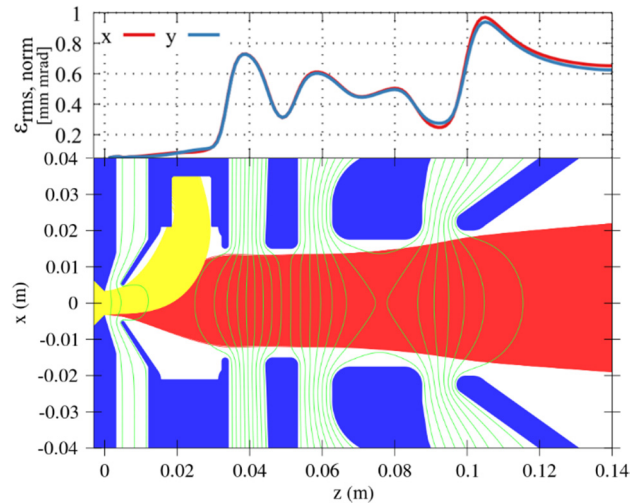


Figure 4: Schematic and emittance evolution of the Linac4's IS03 extraction system at 50 mA beam intensity and an electron to ion ratio of 20. The voltages on the electrodes are (starting from the left) -45kV, -35kV, 0, 30kV, 0.

### Predictions from Simulation

The beam emittance depends on two parameters: the current extracted from the source and the puller-dump voltage. The influence of these parameters was studied using IBSIMU [9]. Figure 5 shows a comparison of measured and simulated emittances for the operational range of the puller-dump voltage. During the measurements, the electron to ion ratio was in the range of 1 to 3. For these values, IBSIMU simulation predicts that the emittance remains almost constant in the range from 8-10 kV, while in the simulation there is a dramatic increase towards lower voltages. We observe, however, that for an artificial e/H ratio of 20, the measured emittance are well reproduced. This applies to all rms beam parameters, and when comparing the dependence of the emittance on the beam current.

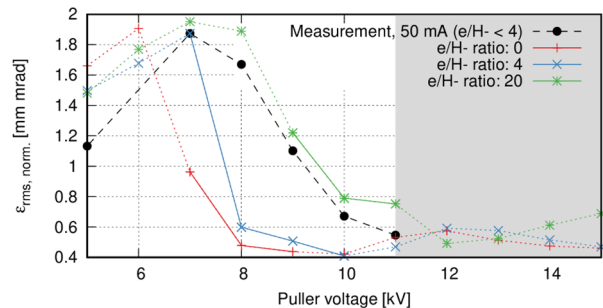


Figure 5: Emittance as a function of puller voltage. Measured data e/H=1-3) and IBSIMU results for different e/H.

Figure 4 shows the evolution of the rms emittance of a 50 mA beam along the system. Since the emittance does not grow significantly until after the electrons are dumped, the differences in emittance for different e/H ratios is not due to aberration caused by the deflected electrons.

However, increasing the current of the co-extracted electrons increases the space charge density in the extraction gap, causing the meniscus to be less and less concave or even convex for higher electron currents. The beam thus

starts with a higher divergence and passes the rest of the extraction system with a larger size. Due the larger filling degree of the electrodes, the result is aberration and emittance growth further downstream. A large fraction of this growth occurs at the end of the puller-dump electrode, which also acts as a focusing lens.

The higher-than-expected emittance of the beam is thus largely due to aberration caused by a shift in meniscus compared to the assumptions. One possible way to improve the beam quality without a radical redesign is to adapt the extraction gap to the rest of the system.

We simulated a variety of changes to the system:

1. Reducing the distance between plasma electrode and puller electrode causes a higher extraction field and thus a more concave meniscus. Predicted improvement in rms emittance for 1 mm shift around 15% between 40 and 60 mA.

Along with option 1:

2. A larger angle on the plasma electrode causes higher electrostatic focussing and thus a smaller beam in the rest of the system. Predicted improvement in rms emittance at 30° instead of 17°, around 15% between 40 and 60 mA.
3. A larger bore causes the meniscus to be more concave. With a diameter of 7.5 mm instead of 6.5 mm, improvements of up to 50 % in the rms emittance at 60 mA are predicted; however, there is no improvement or even a degradation below 40 mA.

### Emittance Results in Volume Mode

All three options were implemented at the test stand and emittances measured in un-caesiated (volume) mode with the idea of testing only the configuration that showed the largest improvement in surface mode.

The control of the emittance meter was automatized using python, making it possible to scan a large number of source settings while recording the beam current and the electron-to-ion ratio.

The emittance measurements contain a signal from particles neutralized in the extraction system. This signal was cut and a noise filter applied, which removes a signal if the sum of the signal in the surrounding area is below a small threshold. The measured rms emittances are plotted in Fig. 6 as a function of beam current.

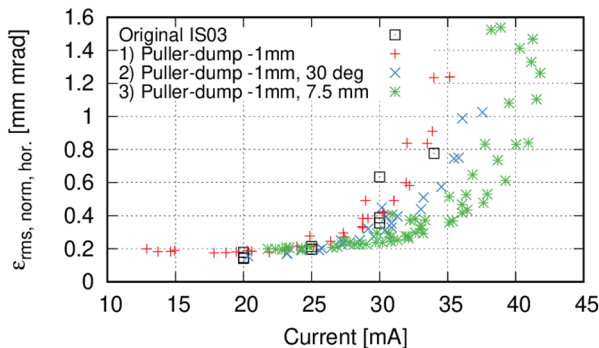


Figure 6: Measured rms emittance for the different electrode configurations. Differences in the electron to ion ratio cause the spread of values at fixed current.

In volume mode, both increasing the angle of the plasma electrode and increasing the plasma bore results in an improvement of the rms emittance and the maximum current, while the movement of the puller-dump electrode shows no clear effect.

Backtracking the measured phase-space distributions of the electrode with 7.5 mm bore diameter and matching these to the acceptance of the RFQ suggests a maximum transmission of up to 32 mA for a source current of 35 mA in volume mode.

### MASK MEASUREMENT RESULTS

As for the emittance measurements, transmission through the mask was measured for a wide range of source parameters. Figure 7 shows the maximum current transmitted through the mask as a function of the current provided by the source. As for the emittance measurements, the spread in transmission at fixed currents is caused by differences in electron to ion ratio. Due to venting of the system during installation of the mask, the electron to ion ratio was larger during the mask measurements, also limiting the currents that could be reached.

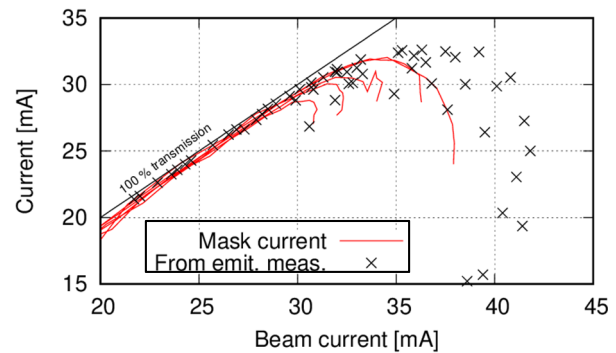


Figure 7: Current through the mask (lines) as a function of the source current in comparison to the current within the RFQ acceptance calculated from emittance measurements.

Both measurement techniques give the same prediction for the RFQ transmission, a maximum of 32 mA for source currents of about 35 mA. In the future, a similar scan will verify the predictions on the Linac4 RFQ.

### CONCLUSION AND OUTLOOK

The measurements of different electrode geometries at the Linac4 test stand have given an important insight on how to improve the current through Linac4 RFQ. The technique of measuring a current passing through a system that reproduces the acceptance of the RFQ has been validated. In the future, it will speed up the qualification of a source for the Linac4 RFQ. The slit-and-grid emittance measurement device allows complementing these information with knowledge of the beam distributions and the time structure along the pulse.

## REFERENCES

- [1] A. Lombardi, "Commissioning of Linac4", these proceedings.
- [2] G. Bellodi, V. A. Dimov, L. Hein, J.-B. Lallement, A. M. Lombardi, O. Midttun, R. Scrivens, P. Posocco, "Linac4 45 keV Proton Beam Measurements", in *Proc. Linac'12*, Tel Aviv, Israel, Sep 2012, paper THPB011, pp.867-869.
- [3] KR. Crandall, TP. Wangler, "PARMTEQ a beam-dynamics code for the RFQ linear accelerator", in Proc. 8th AIP Conference 11/1988; 177(1): 22-28.
- [4] R. Duperrier, "Toutatis: A radio frequency quadrupole code", *Physical review special topics*, Vol. 3, 124201 (2000).
- [5] A. Perrin, JF. Armand, "Travel v4.06 user manual", CERN internal note, 2003.
- [6] TraceWin  
<http://irfu.cea.fr/dacm/logiciels/>
- [7] J. Lettry *et al.*, "Linac4 H<sup>-</sup> ion sources", *Review of Scientific Instruments* 87, 02B139 (2016)
- [8] D. Fink *et al.*, "H<sup>-</sup> Extraction Systems for CERN's Linac4 H<sup>-</sup> Ion Source", *Nuclear Inst. and Methods in Physics Research, A Ms. Ref. No.: NIMA-D-18-00635R1*
- [9] T. Kalvas *et al.*, "IBSIMU: A three-dimensional simulation software for charged particle optics", *Rev. Sci. Instrum.* 81, 02B703, (2010)